Journal of Molecular Liquids 159 (2011) 2–8

Contents lists available at ScienceDirect

Journal of Molecular Liquids

journal homepage: www.elsevier.com/locate/molliq

Rattling the cage: Micro- to mesoscopic structure in liquids as simple as argon and as complicated as water

David A. Turton [a], Johannes Hunger [b], Alexander Stoppa [b], Andreas Thoman [d], Marco Candelaresi [a], Glenn Hefter [c], Markus Walther [d], Richard Buchner [b], Klaas Wynne [a,*]

[a] Department of Physics, SUPA, University of Strathclyde, Glasgow G4 0NG, UK
[b] Institute of Physical and Theoretical Chemistry, University of Regensburg, 93040 Regensburg, Germany
[c] Chemistry Department, Murdoch University, Murdoch, W.A. 6150, Australia
[d] Department of Molecular and Optical Physics, Albert-Ludwigs-Universität Freiburg, 79104 Freiburg, Germany

ARTICLE INFO

Available online 15 May 2010

Keywords:
Ultrafast
Optical Kerr effect
Raman
Terahertz
Dielectric relaxation
Terahertz field-induced second-harmonic generation
Mesoscopic
Fischer clusters
Jamming
Nanoscale
Room-temperature ionic liquids
Water
Electrolyte
Noble gas liquids

ABSTRACT

The water molecule has the convenient property that its molecular polarizability tensor is nearly isotropic while its dipole moment is large. As a result, the low-frequency anisotropic Raman spectrum of liquid water is mostly collision-induced and therefore reports primarily translational motions while the far-infrared (terahertz) and dielectric spectrum is dominated by rotational modes. Atomic and globular–molecular liquids have a zero dipole moment as well as an isotropic polarizability tensor. These spectrum-simplifying properties were exploited in a study of a number of liquids and solutions using ultrafast optical Kerr-effect (OKE) spectroscopy combined with dielectric relaxation spectroscopy (DRS), terahertz time-domain spectroscopy (THz-TDS), and terahertz field-induced second-harmonic generation (TFISH) spectroscopy. For room-temperature ionic liquids (RTILs), liquid water, aqueous salt solutions, noble gas liquids, and globular–molecular liquids it was found that, in each case, surprising structure and/or inhomogeneity is observed, ranging from mesoscopic clustering in RTILs to stretched-exponential dynamics in the noble gas liquids. For aqueous electrolyte solutions it is shown that the viscosity, normally described by the Jones–Dole expression, can be explained in terms of a jamming transition, a concept borrowed from soft condensed matter studies of glass transitions in colloidal suspensions.

1. Introduction

The nanometer scale structuring of liquids is of great importance to an understanding of chemical and biochemical reactions as well as of the thermodynamic properties of liquids. Structure is well known in water as a result of the tetrahedral hydrogen-bond network that is perfect in the crystalline ice Ih phase and perturbed in the liquid phase [1,2]. Changes in the degree and type of local structuring in water [3,4] may give rise to phenomena ranging from multiple crystalline phases to glass formation, and possible liquid–liquid phase transitions [5–11]. Recent studies on room-temperature ionic liquids (RTILs [12,13]) have shown mesoscopic structure that is not liquid crystalline in origin [14–17]. Such RTILs may well form the micelle-like structure that is normally associated with amphiphilic properties. There are hints that such nanoscale aggregation may even occur in molecules as simple as *n*-alcohols [18].

It is widely thought that solutes — in particular charged solutes — can increase or reduce the extent of the structure of the solvent, and are classified in the Hofmeister series as kosmotropes (structure makers) and chaotropes (structure breakers), through their influence on viscosity, and on protein folding and unfolding [19–21]. Mesoscopic structure has been observed in aqueous solutions [22–24] as well as in mixtures [25] by a variety of techniques.

Supercooling and glass formation of liquids has been studied for well over 200 years [26] and is still a very active field. The approach of the glass transition is thought to lead to spatial heterogeneity on increasing length scales and the formation of mesoscopic structure sometimes referred to as Fischer clusters [27,28]. Such behavior can be explained by a locally favored structure that is not the structure corresponding to the global enthalpy minimum [29,30]. For example, in a Lennard–Jones liquid, the locally favored structure is an icosahedron whereas the global minimum enthalpy is achieved for an fcc or hcp lattice [31]. In a few cases, the mesoscopic clustering extends to greater length scales and becomes visible [32,33].

In this short collaborative review, we show that through combining a number of spectroscopic probes and applying these to liquids of varying complexity, a better understanding of the

* Corresponding author.
E-mail address: klaas.wynne@phys.strath.ac.uk (K. Wynne).

0167-7322/$ – see front matter © 2010 Elsevier B.V. All rights reserved.
doi:10.1016/j.molliq.2010.04.005

macroscopic properties can be achieved. In Section 2, the experimental techniques are introduced. Section 3 gives the methodology of simplifying the spectra, and Section 4 applies this approach to aqueous salt solutions allowing a re-interpretation of viscosity in the context of the jamming transition. In Section 5, the OKE spectra of very simplest liquids are shown to reveal surprisingly complex behavior and in Section 6 this is shown to be remarkably similar to that of water, implying a universality of non-exponential translational relaxation.

2. Experimental

One is typically interested in macroscopic properties of liquids such as the structural relaxation, which is related to the flow of liquid under shear stress as measured by its viscosity. The macroscopic property of viscosity is related to microscopic phenomena through the well-known Stokes–Einstein–Debye (SED) equation, which, for a probe particle immersed in a solvent, expresses the orientational relaxation time t_n as [34–37].

$$t_n = \frac{6}{n(n+1)}\frac{V\eta}{k_B T}, \tag{1}$$

where n relates to the type of spectroscopy and is typically 1 or 2, V is the volume of the probe, T the absolute temperature, and η the shear viscosity, which in the simplest cases is given by $\eta \propto \exp(E/k_B T)$. Although originally developed for large probes, the SED equation works surprisingly well for molecular probes to within about an order of magnitude or slightly better. For example, at room-temperature in liquid water, with $n=2$ (appropriate for four-wave mixing spectroscopies), $V = 10^{-3}/(55\,N_a)\,\mathrm{m}^3$ (where N_a is the Avogadro number), $\eta = 1$ cP, and $T = 300$ K, one obtains $t_2 = 7.3$ ps, whereas the anisotropy decay time of the OD-stretch in HOD measured using infrared pump-probe experiments is $t_2 = 2.5$–3 ps [20]. Thus, the structural relaxation timescale is approximately a picosecond corresponding with a frequency of 1 THz. It is for this reason that the terahertz-frequency region is crucial to an understanding of liquids such as water.

There are numerous techniques for measuring terahertz structural relaxation such as dielectric relaxation spectroscopy (DRS), terahertz time-domain spectroscopy (THz-TDS), Fourier-transform infrared spectroscopy (FTIR), inelastic neutron scattering (INS), Raman scattering, etc. All of these techniques essentially measure a two-point correlation function. The techniques of DRS, THz-TDS, and FTIR measure

$$S_{\mathrm{DR}}(t) \propto \langle \mu(0)\mu(t)\rangle, \tag{2}$$

the two-point correlation function of the (permanent) dipole moment [19,38–44] and will be referred to collectively as dielectric relaxation. Anisotropic Raman scattering and optical Kerr-effect spectroscopy (OKE) measure [40,45–50]

$$S_{\mathrm{OKE}}(t) \propto \langle \alpha_{xy}(0)\alpha_{xy}(t)\rangle, \tag{3}$$

the correlation function of the anisotropic part of the polarizability tensor [40,45–49]. The lesser-known technique of terahertz field-induced second-harmonic generation (TFISH) measures

$$S_{\mathrm{TFISH}}(t) \propto \langle \mu(0)\beta(t)\rangle, \tag{4}$$

the correlation function of the (permanent) dipole moment and the hyperpolarizability tensor [51,52]. Finally, Brillouin light, X-ray, and neutron scattering experiments measure [53]

$$S_{\mathrm{Brillouin}}(r,t) \propto \int dR \left\langle \delta[R - R_i(0)]\,\delta\left[R + r - R_j(t)\right]\right\rangle, \tag{5}$$

a two-point correlation function involving position as well as time [53]. Other techniques have been developed that measure higher order correlation functions depending on three or even four time intervals, such as, (infrared) photon echoes and 2D-IR, [54–57] fifth-order spectroscopy, [58–61] and Raman photon echoes [62–64]. Although such higher order techniques can in principle extract more information, generally the depth of analysis is limited by poorer signal-to-noise ratios.

A typical spectrum as measured by one of the two-point correlation function techniques is shown in Fig. 1. In a typical molecular liquid, the spectrum consists of several overlapping broad bands. At the lowest frequency is the structural relaxation or α-relaxation band, which is generally associated with rotational diffusion. At the highest frequencies are librational and vibrational bands, while at intermediate frequencies are bands due to rattling of molecules in the cage of surrounding molecules referred to as β relaxation [38]. In some cases, such as in some room-temperature ionic liquids (RTILs), mesoscopic structure can give rise to an even lower frequency band referred to as sub-α relaxation [16].

The most complete model of relaxation is expected to be provided by mode-coupling theory (MCT) developed and widely applied in studies of glass forming liquids. MCT predicts a critical (singular) temperature T_C typically 15–20% above the glass transition temperature. Above T_C, a low-frequency α relaxation is observed that is diffusive and therefore temperature dependent. This is accompanied by temperature-independent, i.e., non-diffusive or oscillatory fast dynamics. In the supercooled region, the lineshape of the α relaxation is typically stretched (i.e., broadened with respect to a Debye function) but the lineshape and amplitude are temperature-independent above T_C [65–68].

Extending MCT to include the terahertz region is still challenging, and inevitably results in less meaningful fitting models, and we therefore use more conventional but readily interpreted phenomenological models. Even so, the contributions to the low-frequency spectrum are very difficult to disentangle and one of our aims is to identify the individual contributions through simplifying the spectra.

The three experimental techniques used in the work described here are dielectric spectroscopy (DS), optical Kerr-effect spectroscopy (OKE), and terahertz field-induced second-harmonic generation (TFISH).

The experimental setup for the OKE measurements has been described previously [16,69–72] and uses 800-nm 24-fs (FWHM) sech^2 pulses with 8 nJ per pulse at a repetition rate of 76 MHz. The beam is split into pump and probe beams (9:1), which are co-focused by a 10-cm focal length achromat into the sample contained in a 2-mm-pathlength quartz cuvette. The variable pump-probe time delay

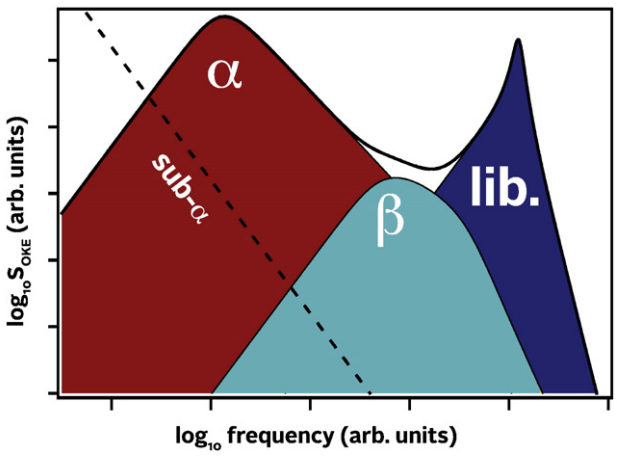

Fig. 1. A typical terahertz-frequency spectrum such as a reduced Raman spectrum or a dielectric relaxation spectroscopy spectrum.

was introduced by an optical delay line with a resolution of 500 nm (3.3 fs). The OKE signal is measured by a balanced-detection technique. For temperature dependent experiments, the samples were condensed into sealed glass cuvettes held in a cryostat (Oxford Instruments, *Optistat DN*) [73].

Typical OKE data in the time-domain is shown in Fig. 2 on double logarithmic axes [72]. The signal in the first few tens of femtoseconds is due to the instantaneous electronic response. This is followed by the rise of librational motions peaking at ~100 fs and fast oscillations due to intramolecular vibrations. The decay at intermediate times (1–10 ps in this case) appears like a power law and reflects β relaxation. Finally, at the longest times (>10 ps in this case) the decay becomes exponential reflecting α relaxation. The inset of Fig. 2 shows a Fourier analysis of the signal, which displays the spectral components of α relaxation (Debye), β relaxation (Cole–Cole), librations, and vibrations [71,72].

Broadband dielectric spectra were obtained by a combination of data from a frequency domain reflectometer using a Hewlett–Packard 85070 M dielectric probe system based on a vector network analyzer (VNA) at 0.2 to 20 GHz, two waveguide interferometers (IFMs) at 27 to 89 GHz, and a transmission/reflection terahertz time-domain spectrometer (THz-TDS) at 0.3 to 3 THz. Far-infrared data were recorded from 0.9 to 12 THz on a Bruker Vertex 70 FTIR spectrometer. Complex permittivity spectra were then derived by Kramers–Kronig transformation [16,19,74].

A typical dielectric spectrum and its comparison with an OKE spectrum over the same range are shown in Fig. 3 [16]. As the dielectric spectrum and the OKE spectrum should show the same dynamics albeit with different strengths for the various components, [40] comparison of the two can give rise to greatly improved fitting. In the case of RTILs, it was found that mesoscopic structure [15,18] gives rise to a sub-α relaxation peak that is very strong in the OKE spectrum but nearly undetectable in the dielectric relaxation spectrum [16].

TFISH measures the correlation function of the dipole moment and the hyperpolarizability [51]. This relatively untried technique has great potential for unraveling these low-frequency spectra. In TFISH, an incoming terahertz pulse aligns dipoles in an initially isotropic sample causing it to become non-centrosymmetric. The decay of the non-centrosymmetry is probed through the second-harmonic generation of a delayed 800-nm probe pulse. As the first field interaction is via the dipole moment, the measured dynamics are expected to be identical to that in DR.

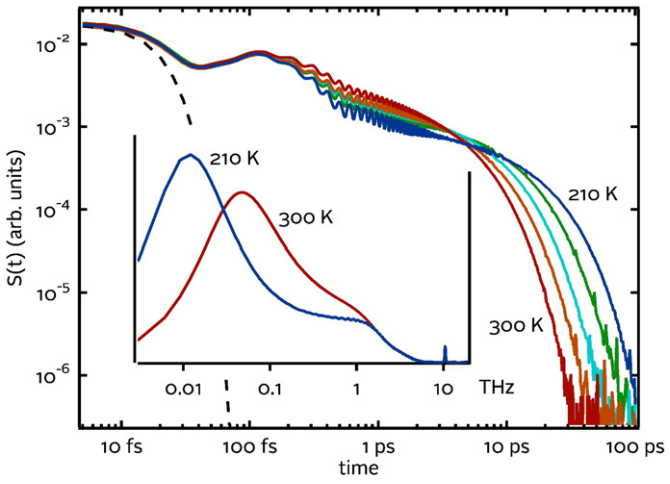

Fig. 2. OKE measurements on trans-1,2-dichloroethene in the time-domain showing, on logarithmic axes, five sets of data measured at 210, 230, 250, 270, and 300 K. The instrument response (autocorrelation) is also shown (dashed). The inset shows the signals at the lowest and highest temperatures in the frequency domain. [72].

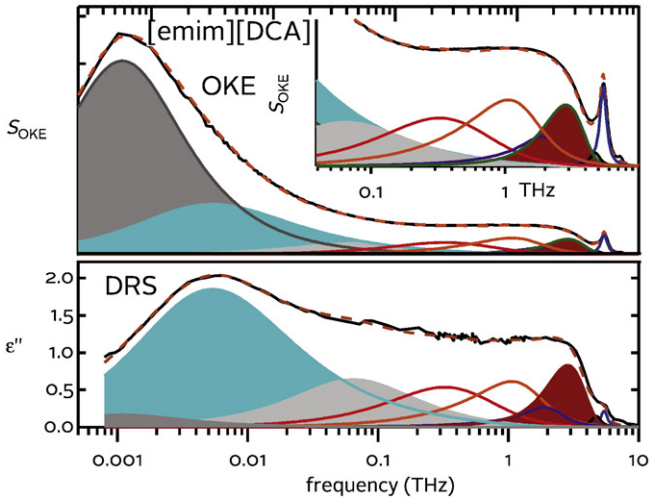

Fig. 3. An OKE spectrum (top) and dielectric spectrum (bottom) of the room-temperature ionic liquid 1-ethyl-3-methylimidazolium dicyanamide (emim DCA). Comparison of the two spectra allows one to identify a sub-α relaxation peak due to mesoscopic structure that is only clearly visible in the OKE spectrum. [16].

3. Simplifying the spectra

At low frequencies, the three types of spectroscopy described here — DR, OKE, and TFISH — all measure rotation of the macroscopic dipole moment or polarizability [46,51]. Thus the spectra have two contributions: from (essentially single-molecule) rotations and librations, and from collision-induced effects [49]. Collision-induced effects were first introduced to explain light scattering from atomic liquids but play a major role in the spectra of all molecular liquids [46,75–77].

The spectra can in principle be simplified if either the permanent dipole moment or the anisotropic part of the polarizability tensor vanishes. Thus, atomic liquids and globular–molecular liquids, by definition, give rise to purely collision-induced spectra. In fact, as atoms obviously cannot rotate, these spectra purely reflect translational motions. Globular–molecular liquids, e.g., carbon tetrachloride, also have purely collision-induced spectra due to the centrosymmetry of the molecules, however, in this case the collision-induced spectrum may have contributions from both translations and rotations (including librations).

In the case of water, the spectra are also simplified: the water molecule has a large permanent dipole moment but an essentially isotropic molecular polarizability tensor (although not because of any intrinsic symmetry) [78]. Therefore, DR spectroscopy is sensitive to diffusive orientational relaxation and a time constant of $t_1/3 = 2.8$ ps is measured [70,79,80] and found to be consistent with the orientational relaxation measured with infrared pump-probe experiments [20]. OKE is insensitive to single-molecule rotational motions and instead measures collision-induced effects due to translational motions of pairs and larger groups of water molecules [70,71]. The OKE decay fits to a Cole–Cole function or a stretched-exponential function with a characteristic timescale of $t_2 = 0.61$ ps [70,71,80]. Thus, OKE spectroscopy measures a β relaxation related to the formation of transient cages in the liquid. Temperature dependent OKE experiments have shown that the β-relaxation process in water slows down as a function of temperature consistent with the predictions of MCT, with a critical temperature $T_c = 221$ K [67].

4. Aqueous salt solutions

Aqueous electrolyte solutions are of particular interest as the influence of the charges on the structure of the surrounding water is still controversial. The surfaces of water-soluble proteins and the

active sites of enzymes are charged and — as often confirmed by X-ray diffraction studies — hold on to water molecules. It has been suggested that the resultant changes in the local structure of water affect the rates of biochemical reactions. Salts also influence the stability of proteins in solution as expressed by the Hofmeister series [19]. It has been suggested that this effect is also due to the influence of the ions on the local structure of the water.

When salts (or sugars) are added to water, the shear viscosity and density generally increase as is, for example, the case with syrup. The attempt to interpret properties of electrolyte solutions at concentrations far from the very dilute region where the Debye–Hückel theory applies has been one of the celebrated failures of physical chemistry [81]. The anomalous concentration dependence of viscosity with solute concentration has not been addressed by a microscopic theory. In the standard picture the viscosity is described by the Jones–Dole expression

$$\eta/\eta_0 = 1 + A\sqrt{x} + Bx, \tag{6}$$

where η/η_0 is the normalized concentration-dependent viscosity, x the salt concentration, and A and B coefficients [82,83]. The Jones–Dole B coefficient is often used to classify ions as either structure makers (kosmotropes) or structure breakers (chaotropes) according to their supposed strengthening or weakening of the hydrogen-bond network of water [84]. Such structural changes appear consistent with changes in viscosity [82] and NMR relaxation timescale [85]. However, infrared pump-probe experiments have indicated that ions have a negligible effect on the structure of water [20,56,86,87].

The ability to measure rotational and translational motions independently in liquid water by using DR and OKE spectroscopy, has been exploited in the study of aqueous salt solutions [70]. The salts NaCl and $MgCl_2$ were chosen since the monatomic ions do not introduce additional dipole moments or anisotropic polarizabilities, thus ensuring that the measured dynamics is entirely due to the water with no contribution from the rotation of the ions.

In the OKE experiments, a rapid slowing down of the dynamics was observed as a function of increasing concentration of $MgCl_2$ (see Fig. 4) [70]. In contrast, in the DR experiments only a very slight variation of the relaxation time is observed combined with a reduction of the static dielectric constant with increasing concentration. This implies that rotational relaxation of water molecules outside the first solvation shells of the ions (as measured in DR experiments) is essentially unaffected while translational relaxation (as measured in OKE experiments) slows down. Both types of experiments observe an increase in the inhomogeneity of the dynamics with concentration, that is, the data indicate that the relaxation is exponential but with an inhomogeneous distribution of decay times. The DR experiments also show that water molecules are immobilized by the cations with, at the highest concentration, approximately seven water molecules immobilized by each Mg^{2+} ion.

The shear viscosity of aqueous salt solutions is generally an increasing function of salt concentration (see Fig. 5). At high concentration, these trends do not follow the Jones–Dole expression Eq. (6) but instead rise more steeply and it is necessary to introduce higher order terms to maintain agreement. Using the Stokes–Einstein–Debye expression Eq. (1), one would expect the rotational relaxation time to increase with viscosity and hence salt concentration but, as Fig. 4 shows, this is not the case.

In the theory of supercooled liquids and glasses, the shear viscosity increases with decreasing temperature [9,38,89,90]. As the glass transition is approached, viscosity diverges away from simple Arrhenius behavior but may be described using the Vogel–Fulcher–Tammann (VFT) equation

$$\eta \propto \exp\left(\frac{DT_0}{T-T_0}\right), \tag{7}$$

where T_0 is the critical temperature corresponding to the glass transition and D is the fragility parameter [91]. The interpretation of the VFT equation is that as the temperature is lowered, the barrier for rearranging the liquid structure increases (due to the increasing extent of cluster formation) resulting in the super-Arrhenius behavior of the temperature dependent viscosity. At the critical temperature, the barrier becomes infinite and the system 'jams' to form a solid-like state.

The concept of jamming also occurs in soft condensed matter physics. For example, a suspension of colloidal particles can jam when a critical concentration of particles is reached. This may be expressed as

$$\eta \propto \exp\left(\frac{A}{\phi-\phi_0}\right), \tag{8}$$

(or similar algebraically diverging expressions derived from mode-coupling theory [92]) where ϕ is the packing fraction and ϕ_0 the critical packing fraction [93]. For monodisperse simple hard spheres, the highest physically achievable packing fraction is $\phi = \pi/\sqrt{18} \cong 0.740$,

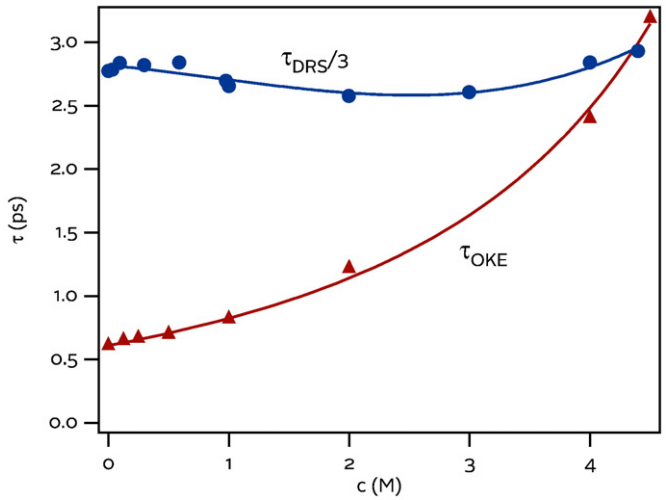

Fig. 4. Relaxation times of aqueous solutions of $MgCl_2$ at 25 ° C obtained using DRS (●) and OKE spectroscopy (▲). The DRS relaxation time has been divided by a factor of 3. The DRS relaxation is associated with rotational motion while the OKE relaxation is associated with translational motions [70].

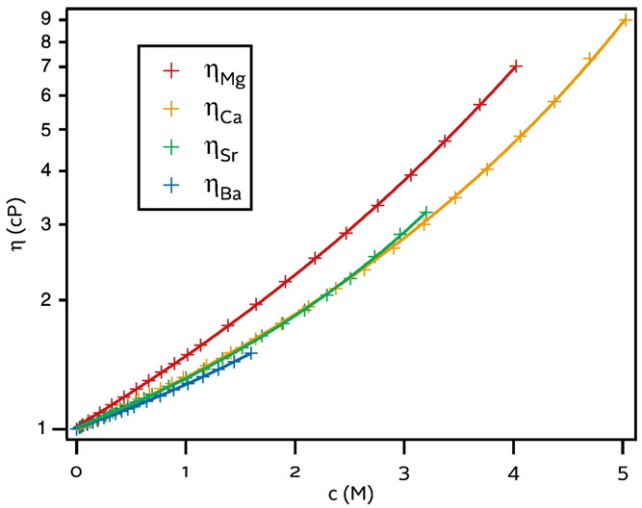

Fig. 5. The macroscopic shear viscosity of aqueous solutions of some divalent cations [88]. In all cases, the anion is chloride. Notice that the viscosity scale is logarithmic.

which occurs for a perfect crystalline fcc or hcp lattice. For a random close-packed hard sphere liquid, jamming occurs at $\phi \cong 0.63$ [94]. The concepts of glass formation and jamming are now generally considered to be equivalent within a model that considers temperature, packing density, and shear force [95–97].

The Mg^{2+} cation considered here holds on tightly to a layer of about 6–7 water molecules. The residence time of these, first solvent shell, water molecules is about 400 ps [98] compared to about 4 ps for water in the first shell around water [99]. Therefore, this cluster with the cation at the center can be considered a (relatively-soft) sphere. As the concentration of the salt increases, so does the concentration of these soft spheres, thus, one may expect a VFT-like dependence of viscosity on salt concentration x, i.e.,

$$\eta \propto \exp\left(\frac{Dx_0}{x - x_0}\right), \tag{9}$$

where x_0 is the jamming concentration. A similar expression for solution conductivity has been suggested previously [81] although without reference to the concept of jamming.

Fig. 5 shows fits with the VFT expression Eq. (9) to the shear viscosity data for four group 2 cations, while Table 1 shows the fit parameters for both divalent and monovalent cations. In each case the critical radius r_0 derived from the jamming concentration x_0 agrees with the cation–OH_2 distance obtained from MD simulations and therefore consistent with the soft-sphere model.

5. Simple liquids

As explained above, the water molecule has a nearly isotropic molecular polarizability tensor allowing the isolation of translational relaxation from rotational relaxation in OKE spectroscopy. The logical next step then is to study molecules with a center of inversion (e.g., methane) or even atoms [105–107]. We have studied the noble gas liquids of argon, krypton, and xenon under the initial assumption that the dynamics would be extremely simple [73].

OKE spectroscopy (as well as anisotropic Raman scattering) is sensitive to the rotation of the polarizability tensor [46,49]. The only anisotropy in the polarizability tensor of atomic liquids comes from collision-induced effects. The first-order collision-induced contribution π on atom j due to other atoms k can be expressed as

$$\pi_j = \alpha_j \cdot \sum_{\substack{k=1 \\ k \neq j}}^{N} T_{jk} \cdot \alpha_k, \tag{10}$$

where α is the isolated-atom polarizability and T_{jk} is the dipole–dipole interaction tensor [49,76]. In atomic liquids, the dipole–dipole tensor is simply $T_{jk} = 1/r_{jk}^3$ where r is the interatomic separation. Thus, the collision-induced spectrum depends on interatomic spacing as r^{-6} to r^{-8} and is therefore essentially due to *nearest neighbor contributions only*. The 'rotation' that is seen in such an experiment is that of an encounter pair undergoing transverse and longitudinal relative motions.

Brillouin scattering experiments can measure the dispersion curves of the acoustic (LA and TA) phonon modes up to the Brillouin zone boundary in crystalline samples. In crystalline argon, the LA and TA phonon frequencies at the zone boundary are 1.6 and 2.1 THz. In disordered materials such as liquids, spatial damping localizes the 'phonons' near the pseudo Brillouin zone (PBZ) where the phonon wavelength becomes equal to the interatomic spacing. As a result, Brillouin scattering cannot resolve phonons near the PBZ.

Normally, Raman scattering (and hence OKE spectroscopy) is only sensitive to acoustic phonons at scattering wavevectors near zero. However, because the Raman (and OKE) scattering intensity is wholly collision-induced in this case, and since this effect falls off so rapidly with interatomic distance, the spectrum now represents the dynamics of (localized) phonons at the PBZ.

The OKE signals of liquid argon, krypton, and xenon near their respective triple points and water at room temperature are shown in Fig. 6. The signals have been rescaled (to the argon signal) to show that — despite the different properties of atomic mass, size, and polarizability — the decay function for the three atomic liquids is identical within the signal-to-noise ratio except for a pair of amplitude and frequency scaling parameters [73]. At times $t/t_x > 1.5$ ps the decay measured is consistent with the derivative of the stretched-exponential function

$$\frac{d}{dt}\exp\left[-(t/\tau)^{\beta}\right], \tag{11}$$

with $\beta = 0.66$ for all three liquids [73]. Around $t/t_x = 1$ ps, weak oscillatory behavior is visible. To fit the data accurately, a pair of oscillatory modes is necessary and the optimum fit was given by a pair of damped harmonic oscillators in addition to Eq. (11) (B1, B2, and S in Fig. 6).

It is well known that the law of corresponding states [108] applies to thermodynamic properties of simple liquids and it was long since demonstrated that the thermodynamic variables and phonon frequencies of noble gas solids are homologous and are related to each other through a scaling factor. Inelastic neutron scattering studies have also shown that the phonon dispersion curves for solid argon,

Table 1
Mono- and divalent cations, their effective jamming radius r_0, the cation-OH_2 distance as obtained from MD simulations $r_{ion\text{-}O}$ (Å), and the first shell residence time τ_{MD}.

Ion	r_0 (Å)	$r_{ion\text{-}O}$ (Å)	τ_{MD} (ps)
Mg^{2+}	2.97	2.1–2.2 [98,100]	422 [98]
Ca^{2+}	3.18	2.4–2.5 [98,100,101]	700 [101]
Sr^{2+}	3.53	2.9 [98]	51 [98]
Ba^{2+}	3.44	–	–
H^+	1.95	–	–
Li^+	2.26	2.0 [98,101,102]	40–100 [98,101–104]
Na^+	2.96	2.4–2.5 [98,100,101]	14.7–34 [98,101,103,104]
K^+	–	2.8–2.9 [98,100,101]	8.2–14 [98,101,103]

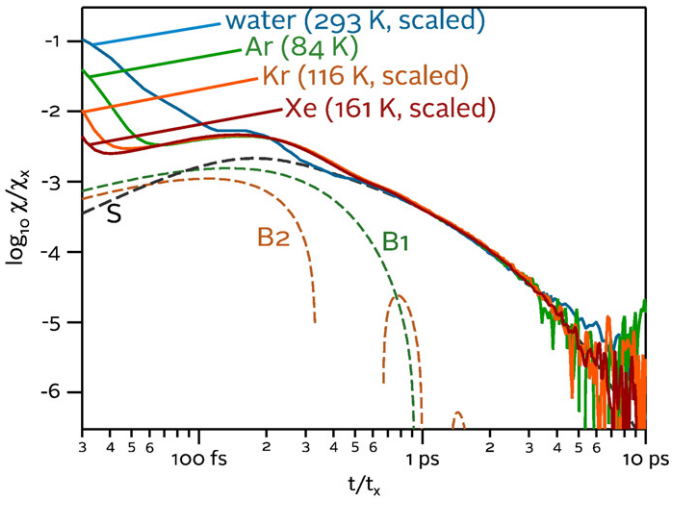

Fig. 6. Time-domain OKE data for liquid xenon, krypton, argon, and water displayed on logarithmic axes. The fit to the xenon data is shown decomposed into two oscillatory functions (B1 and B2) and a stretched-exponential function (S). The xenon, krypton, and water data have been scaled horizontally ($t_x = 0.61$, 0.74, 0.81 respectively) and vertically ($\chi_x = 0.2$, 0.46, 1) to show the universal diffusional decay: all decay according to a stretched-exponential function with $\beta = 0.66$ (~0.6 in water [67]). [73].

krypton, and xenon [109] and liquid neon and argon [110] are scalable. Of all substances, argon, krypton, and xenon best satisfy the criteria for application of the law; here we see that it also applies to the dynamics in the liquid state.

In the case of water, it can be seen that the relaxational decay, over approximately two orders of magnitude in amplitude, exhibits the same stretched behavior as the atomic liquids. In a study of liquid and moderately supercooled water, [67] the OKE relaxation was also found to conform to the derivative of a stretched-exponential function with a very similar stretching parameter of $\beta \approx 0.6$ over the entire temperature range. This similarity suggests that the stretched-exponential decay has a fundamental origin [73].

6. Universal behavior?

For water, the behavior seen at short times appears very different to that of the noble gas liquids. Fig. 7 shows the OKE spectrum of liquid water at room temperature where the translational diffusional (cage-rattling) mode is accompanied by two modes: the hydrogen-bond bend and stretch or, equivalently, the transverse acoustic (TA) and longitudinal acoustic (LA) phonon modes [35,111–114]. For water, with its relatively stiff bonding, these are readily identified. In Fig. 7 one can also see the onset of the water librational band (peaking at ~600 cm^{-1} or ~20 THz), which is of course absent in the noble gas liquids.

The fit to the OKE data for argon, krypton, and xenon also require two phonon-like modes [73]. If these were similar in origin to the TA and LA modes in water, it is reasonable that they would be shifted to lower frequency and softened due to the weaker interactions. The pattern of a stretched-exponential mode with $\beta \approx 0.6$ at low frequency and 'phonon' modes at higher frequency can also be observed in globular–molecular liquids, such as carbon tetrachloride and neopentane (see Fig. 8).

It is not surprising to find complicated dynamics in liquid water, which is known to have strong directional hydrogen bonds and clear indications of structure. It is surprising to see similar dynamics in simple liquids above their melting temperatures. As the OKE signal is collision-induced and due to nearest neighbors, the relaxation dynamics must correspond with the breakup of the local solvent cage. It is remarkable that for a weakly interacting liquid this process is non-exponential and nearly identical to that in water.

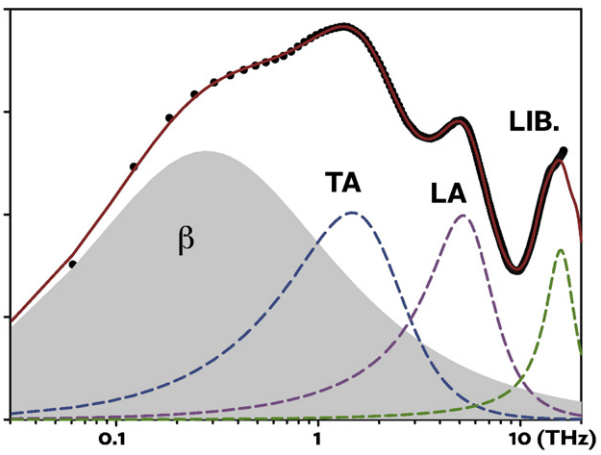

Fig. 7. OKE data for neat water at 25 °C transformed to the frequency domain and deconvoluted. Data (dots), fit (red solid line), and a decomposition of the fit into a cage-rattling β-relaxation mode, two damped harmonic oscillators (corresponding to hydrogen-bond bend and stretch modes), and a harmonic oscillator representing the onset of the librational band [70,71].

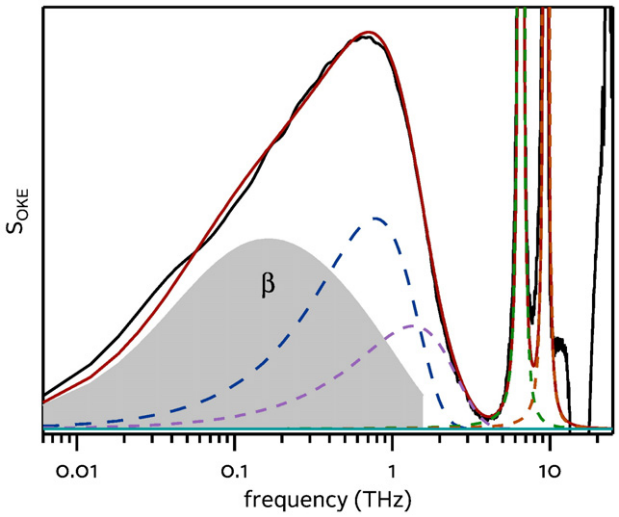

Fig. 8. OKE data for carbon tetrachloride at 25 °C transformed to the frequency domain and deconvoluted. Data (black solid line), fit (red solid line), and a decomposition of the fit into a cage-rattling β-relaxation mode (stretched-exponential decay with $\beta = 0.6$), two anti-symmetrized Gaussian bands, and two harmonic oscillators corresponding to intramolecular vibrational modes.

Acknowledgements

The authors thank Peter Vöhringer for valuable discussion, W. Kunz and H. Helm for laboratory facilities at Regensburg and Freiburg, and acknowledge funding from the U.K. Engineering and Physical Sciences Research Council (EPSRC) and the Deutsche Forschungsgemeinschaft within Priority Program 1191.

References

[1] D. Laage, J. Hynes, Science 311 (2006) 832.
[2] S.T. Roberts, K. Ramasesha, A. Tokmakoff, Acc. Chem. Res. 42 (2009) 1239.
[3] E.B. Moore, V. Molinero, J. Chem. Phys. 130 (2009) 244505.
[4] C. Huang, K.T. Wikfeldt, T. Tokushima, D. Nordlund, Y. Harada, U. Bergmann, M. Niebuhr, T.M. Weiss, Y. Horikawa, et al., Proc. Natl Acad. Sci. USA 106 (2009) 15214.
[5] H. Tanaka, Phys. Rev. B 66 (2002) 064202.
[6] P. Kumar, G. Franzese, H.E. Stanley, J. Phys.-Condens Mat. 20 (2008) 244114.
[7] M. Vogel, Phys. Rev. Lett. 101 (2008) 225701.
[8] C.A. Angell, Science 319 (2008) 582.
[9] C.A. Angell, J. Non-Cryst. Sol. 354 (2008) 4703.
[10] I. Brovchenko, A. Oleinikova, Chemphyschem 9 (2008) 2660.
[11] G.P. Johari, E. Tombari, G. Salvetti, F. Mallamace, J. Chem. Phys. 130 (2009) 126102.
[12] E.W. Castner, J.F. Wishart, H. Shirota, Acc. Chem. Res. 40 (2007) 1217.
[13] H. Weingaertner, Angew. Chem. Int. Edit. 47 (2008) 654.
[14] Q. Kuang, J. Zhang, Z. Wang, J. Phys. Chem. B 111 (2007) 9858.
[15] A. Triolo, O. Russina, H.-J. Bleif, E. Di Cola, J. Phys. Chem. B 111 (2007) 4641.
[16] D.A. Turton, J. Hunger, A. Stoppa, G. Hefter, A. Thoman, M. Walther, R. Buchner, K. Wynne, J. Am. Chem. Soc. 131 (2009) 11140.
[17] O. Russina, A. Triolo, L. Gontrani, R. Caminiti, D. Xiao, L.G. Hines, R.A. Bartsch, E.L. Quitevis, N. Pleckhova, et al., J. Phys.-Condens Mat. 21 (2009) 424121.
[18] A. Triolo, O. Russina, B. Fazio, R. Triolo, E. Di Cola, Chem. Phys. Lett. 457 (2008) 362.
[19] R. Buchner, G. Hefter, Phys. Chem. Chem. Phys. 11 (2009) 8984.
[20] A. Omta, M. Kropman, S. Woutersen, H. Bakker, Science 301 (2003) 347.
[21] N.T. Hunt, L. Kattner, R.P. Shanks, K. Wynne, J. Am. Chem. Soc. 129 (2007) 3168.
[22] M. Sedlak, J. Phys. Chem. B 110 (2006) 13976.
[23] D.L. Sidebottom, Phys. Rev. E 76 (2007) 011505.
[24] L. Porcar, P. Falus, W.-R. Chen, A. Faraone, E. Fratini, K. Hong, P. Baglioni, Y. Liu, J. Phys. Chem. Lett. 1 (2010) 126.
[25] S. Dixit, J. Crain, W. Poon, J. Finney, A. Soper, Nature 416 (2002) 829.
[26] J. Black, Phil. Trans. 65 (1775) 124.
[27] A. Patkowski, T. Thurn-Albrecht, E. Banachowicz, W. Steffen, P. Bosecke, T. Narayanan, E. Fischer, Phys. Rev. E 61 (2000) 6909.
[28] M. Ediger, Annu. Rev. Phys. Chem. 51 (2000) 99.
[29] H. Shintani, H. Tanaka, Nat. Phys. 2 (2006) 200.
[30] H. Shintani, H. Tanaka, Nat. Mater. 7 (2008) 870.
[31] F.C. Frank, Proc. R. Soc. Lond. Ser. A 215 (1952) 43.

[32] R. Kurita, H. Tanaka, Science 306 (2004) 845.
[33] T. Xia, L. Xiao, M. Orrit, J. Phys. Chem. B 113 (2009) 15724.
[34] N.T. Hunt, A.R. Turner, H. Tanaka, K. Wynne, J. Phys. Chem. B 111 (2007) 9634.
[35] K. Winkler, J. Lindner, H. Bursing, P. Vohringer, J. Chem. Phys. 113 (2000) 4674.
[36] N. Hunt, A. Turner, K. Wynne, J. Phys. Chem. B 109 (2005) 19008.
[37] E. Castner, M. Maroncelli, J. Mol. Liquids 77 (1998) 1.
[38] P. Lunkenheimer, U. Schneider, R. Brand, A. Loidl, Contemp. Phys. 41 (2000) 15.
[39] P. Han, X. Zhang, Meas. Sci. Technol. 12 (2001) 1747.
[40] G. Giraud, K. Wynne, J. Chem. Phys. 119 (2003) 11753.
[41] K. Wynne, J. Carey, Opt. Commun. 256 (2005) 400.
[42] D.F. Plusquellic, K. Siegrist, E.J. Heilweil, O. Esenturk, Chemphyschem 8 (2007) 2412.
[43] C. Schmuttenmaer, Chem. Rev. 104 (2004) 1759.
[44] M. Beard, G. Turner, C. Schmuttenmaer, J. Phys. Chem. B 106 (2002) 7146.
[45] M. Cho, M. Du, N. Scherer, G. Fleming, S. Mukamel, J. Chem. Phys. 99 (1993) 2410.
[46] C. Fecko, J. Eaves, A. Tokmakoff, J. Chem. Phys. 117 (2002) 1139.
[47] N.T. Hunt, A.A. Jaye, S.R. Meech, Phys. Chem. Chem. Phys. 9 (2007) 2167.
[48] Q. Zhong, J.T. Fourkas, J. Phys. Chem. B 112 (2008) 15529.
[49] S. Ryu, R. Stratt, J. Phys. Chem. B 108 (2004) 6782.
[50] H. Shirota, T. Fujisawa, H. Fukazawa, K. Nishikawa, Bull. Chem. Soc. Jpn 82 (2009) 1347.
[51] D. Cook, J. Chen, E. Morlino, R. Hochstrasser, Chem. Phys. Lett. 309 (1999) 221.
[52] J. Chen, P. Han, X.-C. Zhang, Appl. Phys. Lett. 95 (2009) 011118.
[53] J.-B. Suck, Condens Matter Phys. 11 (2008) 7.
[54] R.M. Hochstrasser, Proc. Natl Acad. Sci. USA 104 (2007) 14190.
[55] N.T. Hunt, Chem. Soc. Rev. 38 (2009) 1837.
[56] M.D. Fayer, D.E. Moilanen, D. Wong, D.E. Rosenfeld, E.E. Fenn, S. Park, Acc. Chem. Res. 42 (2009) 1210.
[57] S. Garrett-Roe, P. Hamm, Acc. Chem. Res. 42 (2009) 1412.
[58] O. Golonzka, N. Demirdoven, M. Khalil, A. Tokmakoff, J. Chem. Phys. 113 (2000) 9893.
[59] L. Kaufman, J. Heo, L. Ziegler, G. Fleming, Phys. Rev. Lett. 88 (2002) 207402.
[60] C.J. Milne, Y.L. Li, T.L.C. Jansen, L. Huang, R.J.D. Miller, J. Phys. Chem. B 110 (2006) 19867.
[61] Y.L. Li, L. Huang, R.J.D. Miller, T. Hasegawa, Y. Tanimura, J. Chem. Phys. 128 (2008) 234507.
[62] M. Muller, K. Wynne, J. Vanvoorst, Chem. Phys. 128 (1988) 549.
[63] M. Muller, K. Wynne, J. Vanvoorst, Chem. Phys. 125 (1988) 225.
[64] D. Vandenbout, L. Muller, M. Berg, Phys. Rev. Lett. 67 (1991) 3700.
[65] W. Gotze, L. Sjogren, Rep. Prog. Phys. 55 (1992) 241.
[66] S. Wiebel, J. Wuttke, New J. Phys. 4 (2002) 56.
[67] R. Torre, P. Bartolini, R. Righini, Nature 428 (2004) 296.
[68] W. Schirmacher, H. Sinn, Condens Matter Phys. 11 (2008) 127.
[69] G. Giraud, J. Karolin, K. Wynne, Biophys. J. 85 (2003) 1903.
[70] D.A. Turton, J. Hunger, G. Hefter, R. Buchner, K. Wynne, J. Chem. Phys. 128 (2008) 161102.
[71] D.A. Turton, K. Wynne, J. Chem. Phys. 128 (2008) 154516.
[72] D.A. Turton, D.F. Martin, K. Wynne, Phys. Chem. Chem. Phys. 12 (2010) 4191.
[73] D.A. Turton, K. Wynne, J. Chem. Phys. 131 (2009) 201101.
[74] J. Hunger, A. Stoppa, A. Thoman, M. Walther, R. Buchner, Chem. Phys. Lett. 471 (2009) 85.
[75] J. Bucaro, T. Litovitz, J. Chem. Phys. 54 (1971) 3846-&.
[76] D. Frenkel, J. Mctague, J. Chem. Phys. 72 (1980) 2801.
[77] G. Johari, J. Non-Cryst. Sol. 307 (2002) 114.
[78] W. Murphy, J. Chem. Phys. 67 (1977) 5877.
[79] R. Buchner, J. Barthel, J. Stauber, Chem. Phys. Lett. 306 (1999) 57.
[80] T. Fukasawa, T. Sato, J. Watanabe, Y. Hama, W. Kunz, R. Buchner, Phys. Rev. Lett. 95 (2005) 197802.
[81] C. Angell, R. Bressel, J. Phys. Chem.-Us 76 (1972) 3244.
[82] H. Jenkins, Y. Marcus, Chem. Rev. 95 (1995) 2695.
[83] J. Jiang, S. Sandler, Ind. Eng. Chem. Res. 42 (2003) 6267.
[84] R. Mancinelli, A. Botti, F. Bruni, M.A. Ricci, A.K. Soper, Phys. Chem. Chem. Phys. 9 (2007) 2959.
[85] R. Struis, J. Debleijser, J. Leyte, J. Phys. Chem.-Us 93 (1989) 7943.
[86] Y.L.A. Rezus, H.J. Bakker, Proc. Natl Acad. Sci. USA 103 (2006) 18417.
[87] Y.L.A. Rezus, H.J. Bakker, Phys. Rev. Lett. 99 (2007) 148301.
[88] Handbook of Chemistry and Physics, CRC Taylor and Francis, 2006.
[89] C. Angell, K. Ngai, G. Mckenna, P. Mcmillan, S. Martin, J. Appl. Phys. 88 (2000) 3113.
[90] P. Debenedetti, F. Stillinger, Nature 410 (2001) 259.
[91] C. Angell, Chem. Rev. 102 (2002) 2627.
[92] G. Brambilla, D. El Masri, M. Pierno, L. Berthier, L. Cipelletti, G. Petekidis, A.B. Schofield, Phys. Rev. Lett. 102 (2009) 085703.
[93] K. Watanabe, H. Tanaka, Phys. Rev. Lett. 100 (2008) 158002.
[94] J. Mattsson, H.M. Wyss, A. Fernandez-Nieves, K. Miyazaki, Z. Hu, D.R. Reichman, D.A. Weitz, Nature 462 (2009) 83.
[95] A. Liu, S. Nagel, Nature 396 (1998) 21.
[96] Z. Zhang, N. Xu, D.T.N. Chen, P. Yunker, A.M. Alsayed, K.B. Aptowicz, P. Habdas, A.J. Liu, S.R. Nagel, et al., Nature 459 (2009) 230.
[97] R. Mari, F. Krzakala, J. Kurchan, Phys. Rev. Lett. 103 (2009) 025701.
[98] S. Obst, H. Bradaczek, J. Phys. Chem.-Us 100 (1996) 15677.
[99] D. Laage, J.T. Hynes, Proc. Natl Acad. Sci. USA 104 (2007) 11167.
[100] D. Jiao, C. King, A. Grossfield, T.A. Darden, P. Ren, J. Phys. Chem. B 110 (2006) 18553.
[101] S. Koneshan, J. Rasaiah, R. Lynden-Bell, S. Lee, J. Phys. Chem. B 102 (1998) 4193.
[102] D. Spangberg, R. Rey, J. Hynes, K. Hermansson, J. Phys. Chem. B 107 (2003) 4470.
[103] E. Guardia, D. Laria, J. Marti, J. Phys. Chem. B 110 (2006) 6332.
[104] K. Moller, R. Rey, M. Masia, J. Hynes, J. Chem. Phys. 122 (2005) 114508.
[105] W. Lotshaw, D. Mcmorrow, N. Thantu, J. Melinger, R. Kitchenham, J. Raman Spectrosc. 26 (1995) 571.
[106] M. Khalil, O. Golonzka, N. Demirdoven, C. Fecko, A. Tokmakoff, Chem. Phys. Lett. 321 (2000) 231.
[107] N. Boeijenga, A. Pugzlys, T. Jansen, J. Snijders, K. Duppen, J. Chem. Phys. 117 (2002) 1181.
[108] E.A. Guggenheim, J. Chem. Phys. 13 (1945) 253.
[109] V. Ramamurthy, S. Rajendraprasad, J. Chem. Phys. 83 (1985) 3590.
[110] A. Vanwell, L. Degraaf, Phys. Rev. A 32 (1985) 2396.
[111] E. Castner, Y. Chang, Y. Chu, G. Walrafen, J. Chem. Phys. 102 (1995) 653.
[112] G. Walrafen, J. Phys. Chem.-Us 94 (1990) 2237.
[113] K. Winkler, J. Lindner, P. Vohringer, Phys. Chem. Chem. Phys. 4 (2002) 2144.
[114] H. Shirota, E.W. Castner, J. Chem. Phys. 125 (2006) 034904.